Mechanisms for Thermally Enhanced Target Coupling by Repetitively Pulsed Lasers

E. J. Jumper*
Air Force Institute of Technology, Wright-Patterson Air Force Base, Ohio
J. P. Jackson†
KAMAN Sciences Corporation, Colorado Springs, Colorado
J. R. Couick‡ and L. L. McKee§
Air Force Institute of Technology, Wright-Patterson Air Force Base, Ohio
and
C. L. Bohn¶ and M. L. Crawford¶
United States Air Force Academy, Colorado Springs, Colorado

This paper describes the results of computations of the heat and mass transfer to and from an aluminum target when irradiated by an intense 10.6 μm laser pulse, for the case when a laser-supported detonation (LSD) wave is ignited. The results of the computations are compared to an experiment performed by Maher and Hall where a thermal-coupling coefficient of 17.5% was observed. The computations indicate that convective and radiative heat transfer alone are unable to explain the high thermal coupling; vapor recondensation is also investigated as a possible mechanism for explaining the observed coupling coefficient, and does appear to be compatible with the observations. Conclusions are drawn about the possible physical mechanisms at work both during the early phases of the pulse and during the time the LSD wave propagates away from the target.

I. Introduction

WHEN a pulsed laser interacts with a metal target, a fraction of the laser energy is coupled into the target where it resides as stored thermal energy. It has been observed[1,2] (in the case of 10.6 μm pulsed laser-target interactions) that the fraction can increase when a laser absorption wave (LAW) is ignited. This LAW can take on two forms: a laser-supported combustion wave or a laser-supported detonation (LSD) wave. Various researchers have suggested that this enhanced coupling is due to efficient transfer of heat from the LAW to the target via convective heat transfer[2,3] and/or radiative heat transfer.[4] A good summary overview may be found in Ref. 3.

In previous works, two of the authors examined the viability of heat transfer (convective and radiative) being the cause of the enhanced coupling for well-documented cases of 10.6 μm beams interacting with aluminum targets when an LSD wave was ignited.[5,6] The result of these studies indicated that heat transfer did not seem likely as the cause of the observed enhanced thermal coupling in these LSD cases. At that time an alternative hypothesis was proposed to account for the enhancement—target-vapor recondensation.

This paper attempts to build a stronger case for the viability and importance of the vapor-recondensation mechanism in laser-target interactions where LSD waves are ignited. The paper describes a more recent study that investigated in greater detail both the convective heat-transfer problem and the expected effect of vapor recondensation. Plasma reradiation is also treated in a conservative sense to assess its contribution to the enhanced coupling. Finally, an overview is given of the relative role of each mechanism as a function of time.

II. Experimental Background

Although there are a large number of experimental studies that have demonstrated the enhanced thermal-coupling phenomena,[1-3] Maher and Hall[1] have the most useful data set for the purpose of this study. In particular, for the case of a 10.6 μm, 9.3 J laser pulse irradiating an aluminum target, Maher and Hall give not only the final thermal energy residing in the target, but also the radial distribution of that energy. Along with these data is given the details of the pulse shape (temporal), beam quality (spatial), and target dimensions and material. As such, this experiment forms an excellent background against which theoretical predictions may be compared. Information concerning the character of the Maher and Hall pulse is summarized in Fig. 1. The reported coupling coefficient (i.e., percent of beam energy residing in the target) for this 9.3 J experiment was 17.5%.

III. Fluid-Dynamic Computational Environment

The fluid-dynamic framework of the present study was a modified, three-dimensional but radially symmetric, Eulerian (i.e., inviscid, control volume) fluid-dynamic computer program based on the finite-differenced, "flux-divergent" form of the equations for continuity, momentum, and energy. The unmodified program is extensively described elsewhere.[7,8] The thermodynamic and transport properties for high-temperature air were improved somewhat over those used in Ref. 7 to better account for dissociation and ionization effects.[8] Additionally, a separate program was written to compute the viscous/boundary-layer interaction of the fluid with the target boundary based on information output from the Eulerian program. The effect of the evolved target-vapor interaction with the target surface was also handled in the viscous program by selecting an appropriate computational option. Finally, the contribution to the enhanced thermal coupling due to radiation from the plasma to the target was handled separately, also using the flowfield properties provided by the Eulerian program.

Presented as Paper 86-1075 at the AIAA/ASME 4th Fluid Mechanics, Plasma Dynamics and Lasers Conference, Atlanta, GA, May 12-14, 1986; received May 29, 1986; revision received Aug. 8, 1986.

*Professor, Department of Aeronautics and Astronautics. Associate Fellow AIAA.
†Research Scientist, Directed Energy Program. Member AIAA.
‡Presently, Research Engineer, Air Force Weapons Laboatory, Kirtland AFB, NM.
§Assistant Professor, Department of Engineering Physics.
¶Associate Professor, Department of Physics.

In order to understand the rationale for the theoretical treatment that follows, it is helpful to examine the inviscid flowfield as computed by the Eulerian program. The kind of information available from the program output for conditions similar to those of the present study is illustrated in Fig. 2 for a series of times.[7,9] Of interest to this study is the flowfield information in the immediate vicinity of the target boundary. Figure 3 shows the radial velocity distribution as a function of time for the problem under study (i.e., the Maher and Hall experiment[1]) and Fig. 4 gives the temperature distributions. As will be discussed below, correlation of the velocity and temperature curves of Fig. 3 and 4 reveals that, for the purposes of heat-transfer calculations, the important and largest contributing portion of the flowfield is nicely approximated by a three-dimensional stagnation-point flow.

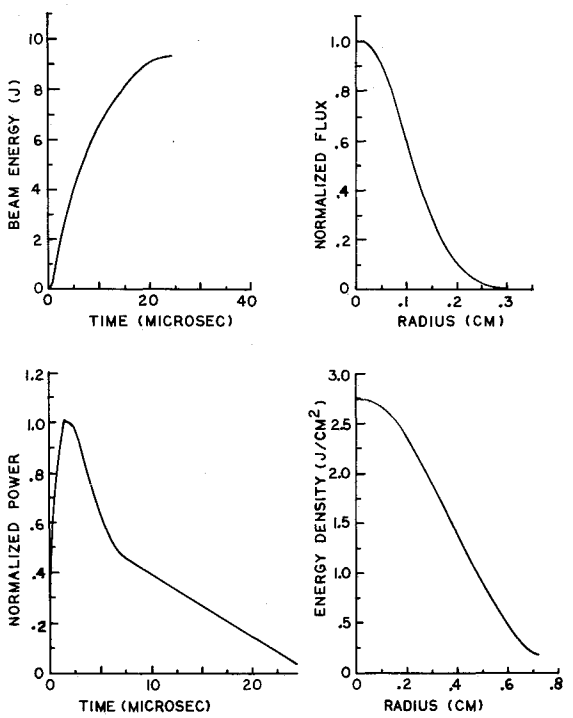

Fig. 1 Characteristics of the Maher and Hall 10.6 μm, 9.3 J laser pulse (the lower right-hand curve shows the energy distribution left in the target at the end of the experiment).

IV. Theoretical Treatment and Physical Assumptions

Heat Transfer (Viscous Interaction)

Since the larger computational environment for computing the overall flowfield properties as a function of time was an inviscid program[7] (cf above), it treated the target boundary as a no-flow-penetration condition. The flow properties furnished by the Eulerian program at a target boundary were used as outer boundary conditions for a viscous boundary-layer analysis. As mentioned above, examination of the flow parameters of Figs. 3 and 4 suggested the use of a relatively simple model for treating the boundary layer; the viscous problem was treated as a pseudosteady stagnation flow using the Eckert reference-enthalpy method.[10-12] Since the reference-enthalpy method has gained universal acceptance for treating high-speed, high-temperature, compressible flows with fluid property variation and chemical dissociation, we need justify here only the interpretation of the flow as being stagnation flow and pseudosteady.

Stagnation-Flow Assumption

The classical three-dimensional stagnation flow at a boundary has a radial velocity distribution of[13]

$$U_r = ar \tag{1}$$

where U_r is the radial component of the velocity just outside the boundary layer (i.e., the velocity determined by the Eulerian program at the wall cells of the computational grid, as a function of time), a the "relaxation" constant, and r the radial position with respect to the center of the laser beam. It is clear from the shape of the curves in Fig. 3 that the flowfield approximates a three-dimensional stagnation point, according to the requirements of Eq. (1), out to the point of peak velocity. Further, one can extract the relaxation coefficient a from information such as displayed in Fig. 3. This has been done and is shown in Fig. 5. It can be seen that the flowfield not only closely approximates that of a three-dimensional flowfield, but also is almost unchanging out to approximately

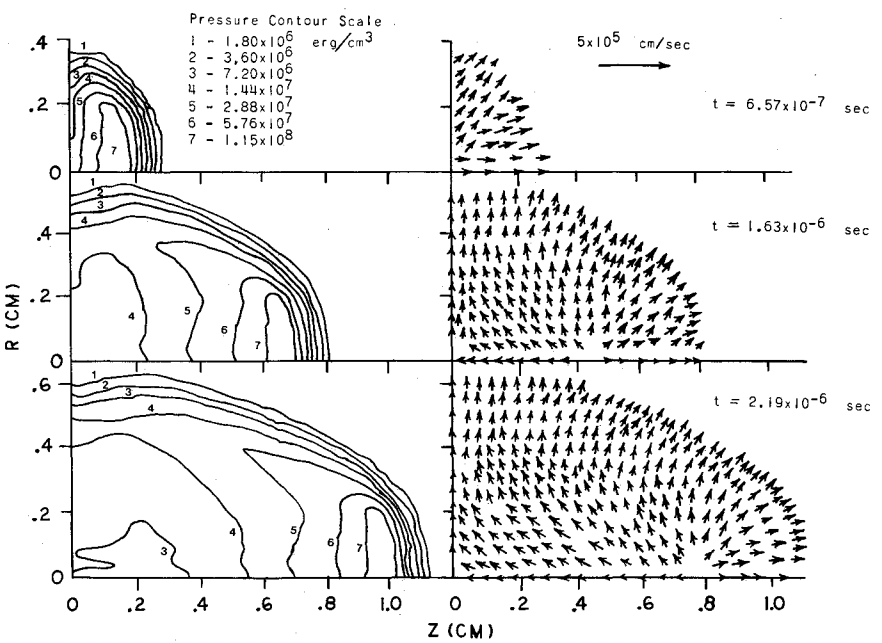

Fig. 2 Example output from the Eulerian program for a 10.6 μm, 0.22 cm radius, 10^7 W/cm² beam on an aluminum target. Shown are the pressure and velocity fields at three times associated with the propagation of an LSD wave (adapted from Ref. 9).

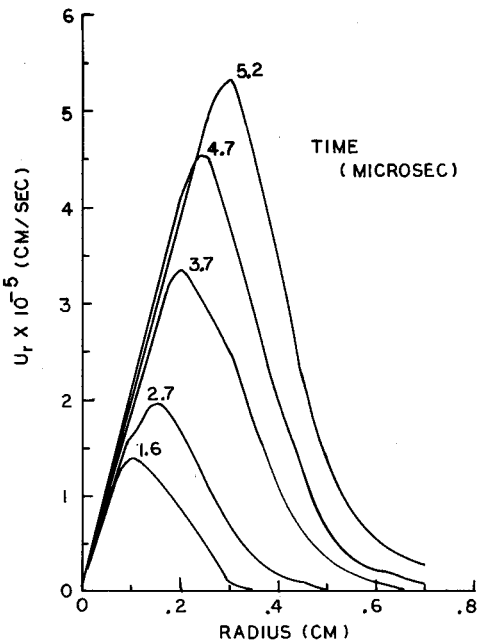

Fig. 3 Radial velocity field at the target boundary computed by Eulerian program at various times for the Maher and Hall experiment.

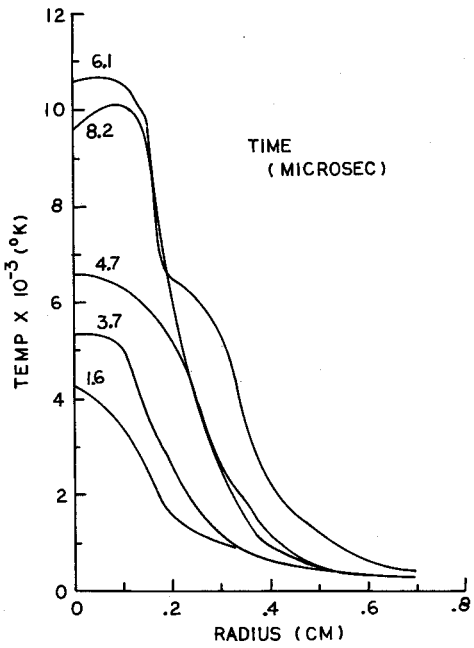

Fig. 4 Temperature field at the target boundary, computed by Eulerian program at various times for the Maher and Hall experiment.

5 μs, then decreasing over characteristic times on the order of 5 μs. These times are useful in assessing the validity of the pseudosteady assumption.

Pseudosteady Assumption

There are three things which may be stated as conditions that should be checked in order to justify the use of the pseudosteady assumption for the purpose of analyzing the Maher and Hall experiment[1]: 1) the three-dimensional stagnation flowfield must develop rapidly compared to the time of the experiment; 2) the transients involved in setting up the viscous boundary layer should be rapid compared to the time of the experiment; and 3) once established, the rate at which the three-dimensional flowfield changes should be relatively slow compared to the time required for the boundary layer to

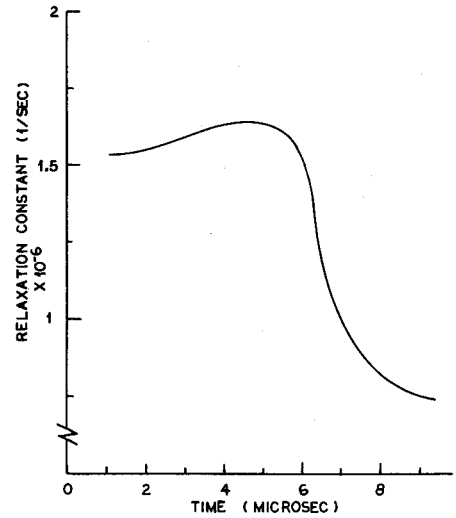

Fig. 5 Radial-velocity-field relaxation coefficient for Eq. (1) extracted from computational results similar to Fig. 3 for the Maher and Hall experiment.

adjust. If these conditions are met, one can expect that the results obtained using the pseudosteady assumption represent a reasonable simulation of the convective heat transfer for the Maher and Hall experiment.

The time to establish the viscous boundary layer (which, because the Prandtl number is on the order of 1.0, is the same order of time required to establish the thermal boundary layer) may be approximated by estimating the boundary-layer thickness and the time it takes for a boundary disturbance to diffuse that distance. The boundary-layer thickness may be approximated for stagnation flow by[13]

$$\delta \cong \frac{1.98}{(a/\nu)^{1/2}} \tag{2}$$

where a is again the relaxation coefficient, δ the boundary-layer thickness, and ν the kinematic viscosity. For the Maher and Hall experiment, Eq. (2) gives a δ on the order of 1.0×10^{-2} cm. The time for a boundary disturbance to propagate this distance may be estimated by[13]

$$t \cong \delta^2/4\nu \tag{3}$$

According to Eq. (3), this time is less than 1 μs. Thus, the requirement that this time be small compared to the time of the experiment appears to be met. Further, this is the time required to establish the boundary layer completely. Adjustments to the flowfield boundary conditions over the times shown in Fig. 5 can be considered to be slow when compared to the boundary-layer adjustment times.

Taken together, it would appear that the conditions required to justify the use of the pseudosteady analysis have been met for the Maher and Hall experiment.[1]

Reference-Enthalpy Method

According to Eckert,[10] the convective heat-transfer coefficient for a three-dimensional stagnation flow may be found from the "enthalpy" Nusselt number Nu_i determined by

$$Nu_i = 0.763\,(Pr)^{0.4}\,(Re)^{0.5} \tag{4}$$

where Pr is the Prandtl number and Re the Reynolds number given, respectively, by

$$Nu_i = c_p h_i r/k \tag{5}$$

$$Pr = c_p \mu/k \tag{6}$$

$$Re = U_e r/\nu \tag{7}$$

where c_p is the specific heat, h_i the "enthalpy" convective heat-transfer coefficient [i.e., the heat flux is determined using an enthalpy difference rather than a temperature difference,[10] cf Eq. (9)], μ the viscosity, k the thermal conductivity, U_e the local velocity just outside the boundary layer, and ν the kinematic viscosity. The properties are evaluated at the reference enthalpy temperature T_{ref}, which is consistent with the reference enthalpy i_{ref} given by

$$i_{\text{ref}} = i_e + 0.5(i_w - i_e) + 0.22(i_r - i_e) \tag{8}$$

where i_e is the enthalpy just outside the boundary layer, i_w the enthalpy of the fluid evaluated at the wall temperature, and i_r the enthalpy of the fluid evaluated at the recovery temperature. The heat flux to the wall $\dot{Q}_T$ is then determined by

$$\dot{Q}_T = h_i(i_r - i_w) \tag{9}$$

Vapor Condensation

It is known that accompanying the ignition of an LSD wave is the evolution of target vapor[3,14]; what is not clear is the amount of vapor evolved prior to ignition. As will be discussed in Secs. V and VI, it is possible to argue that, in those cases were an LSD wave is ignited, "apparent" absorptivities of nearly 100% may be associated with the evolution of vapor (although, as will be discussed below, the absence of sufficient evolved vapor may yield target absorptivities normally experienced in the absence of ignition of LAW's). The vaporization process removes energy from the target that would otherwise have been captured by the target in the form of thermal energy. As the vapor leaves, it removes its latent heat of vaporization L_v. The reverse process is also possible; therefore, if the target vapor recondenses onto the target, it redeposits this energy back into the target along with its random kinetic energy and, depending on the surface temperature, latent heat of sublimation L_m.

The mechanism for vapor condensation is the microscopic kinetic impacts of vapor atoms on the target, which is due to their presence in the vicinity of the target boundary by virtue of the contribution that the target-vapor partial pressure makes to the pressure of the gas mixture. It is known that virtually every kinetic impact of the metal atoms with the target bonds to the target.[15] A conservative estimate of the rate of energy deposition due to vapor condensation may be computed as follows. The kinetic rate of impact (impingement) per unit area $\dot{N}$ is given by[16]

$$\dot{N} = n(kT/2\pi m)^{1/2} \tag{10}$$

where n is the number density of the vapor atoms, k the Boltzmann constant, T the absolute temperature, and m the mass of the metal atom. The energy flux $\dot{Q}_V$ into the target may be conservatively estimated by

$$\dot{Q}_V = \dot{N}m[L_v + c_{pm}(T_v - T_m) + L_m] \tag{11}$$

where c_{pm} is the specific heat of the molten metal, T_v the vaporization temperature, and T_m the melt temperature. Equation (11) assumes that the surface temperature is less than the melt temperature. If the surface is hotter than the melt temperature, T_m should be replaced with the surface temperature T_s and L_m should be eliminated; the hottest the surface may be is T_v. Equation (11) may then be used to compute the heat flux to the target as a function of position using the number density of the vapor at the wall.

Without a detailed treatment of the mass boundary layer, the number density at the wall is not available. In such a detailed treatment, Eq. (10) would form a gradient boundary condition at the wall and the Eulerian-furnished number density would be the outer boundary condition for the mass boundary layer; however, because so little is known about the details of the evolution of the target vapor (cf Sec. VI), a detailed treatment of the mass boundary layer is neither warranted at this time nor likely to give any better results for the present purposes than a simpler approach. This, in the absence of a mass boundary-layer treatment, the impingement rate of Eq. (10) and subsequent heat flux may be approximated by using the number density furnished by the Eulerian program; it is, however, appropriate to assess the effect of this approximation.

The use of the Eulerian-furnished number density rather than a full mass boundary-layer treatment can be argued to be that of either too small or too large a number density. The argument for being too small is as follows. The number density of vapor in the surface cell is based on the amount of vapor evolved from the target and is assumed to be uniformly dispersed into the cell forming a partial pressure of that cell. In fact, the diffusion times are long compared to the time of the experiment. Thus, as it is evolving, the vapor forms a gradient (mass transport boundary layer of thickness δ_m), with the vapor partial pressure at the wall being closer to that of the cell pressure and decreasing to a small fraction of the cell pressure at a distance from the wall on the order of the mass transport boundary-layer thickness. On the other hand, after the vapor begins to recondense, the reverse process takes place—i.e., the vapor is depleted at the wall and must be replenished by diffusion. Thus, an argument can be made that the Eulerian-furnished n is too large.

Of these arguments, the first probably dictates whether the computation is conservative or optimistic (i.e., furnishes a lower or upper bound, respectively, on the expected target-heating rates due to vapor condensation) for the following reason. If the rate of evolution of vapor is the same as the rate at which vapor is depleted by condensation, then the initial underestimate of n will be compensated for by the overestimate of n in the reverse problem. However, the compensation will be equitable only if the half-cell height is on the order of the boundary-layer thickness, which calls for a computation that is neither conservative nor optimistic. In fact, the boundary-layer thickness is an order of magnitude less than the cell height. Thus, the Eulerian-furnished n will tend to underestimate the actual n that might be expected at the edge of the boundary layer. This consideration alone means that the computation should yield conservative energy deposition rates. However, the computation is further driven toward conservatism (i.e., underestimating the potential heat transfer due to vapor condensation) by the fact that the vapor is evolved more rapidly than it condenses. In fact, the vapor evolves so rapidly that there is a macroscopic vapor velocity away from the target, so that the partial pressure of the vapor makes up the total gas pressure at the target and is actually higher than the pressure predicted by the Eulerian program during the time of maximum vapor evolution.

Finally, it should be mentioned that the kinetic velocity, i.e., the radical term of Eq. (10), was computed using the temperature furnished by the Eulerian program; in fact, the wall temperature would be more appropriate. As such, the kinetic velocity was overestimated; however, the choice of the Eulerian-furnished temperature rather than the wall temperature was intentional because the number density used was also that furnished by Eulerian program. As such, the number density was consistent with the pressure and temperature of the Eulerian-furnished parameters. Since, for a given pressure, the number density scales directly as the inverse of temperature, the use of the Eulerian-furnished number density more than compensates for the use of the Eulerian-furnished temperature in the computation of the kinetic velocity that scales only by the square root of the temperature. Again, this argues for a conservative estimation of the effect of vapor recondensation.

Radiation

The contribution to the enhanced thermal coupling due to reradiation from the plasma to the target has been computed by others.[5,17] Both of these theoretical studies concluded that

the contribution to enhanced thermal coupling for the case under study was less than 1%. Further, the computations were considered to overestimate the actual contribution due to the fact that most of the plasma reradiation was expected to be in the far ultraviolet[18] and would be severely attenuated in air at temperatures below approximately 1200 K; such attenuation was not accounted for in these studies. What many have interpreted as a contradictory conclusion (cf below) was reached in an experimental study of the role of radiation in enhanced thermal coupling[4]; these authors concluded that most, if not all, of the observed enhanced thermal coupling for their experiment could be accounted for by the *measured* radiant fluence on the target from the plasma. In light of this apparent contradiction, an estimate of the contribution of radiation to the measured thermal coupling was made for both the experiment under study and the experiment of Ref. 4.

The estimate was made in two ways. First, an estimate was made assuming that the plasma was optically thin. In such a case, the radiation would be due to recombination or Bremsstrahlung radiation and an estimate of the volumetric rate of radiation was made after Dawson[19] as

$$\dot{f} = 4.86 \times 10^{-31} D n_e^2 T^{1/2} \tag{12}$$

where $\dot{f}$ is the volumetric rate (emission coefficient) in watts per cubic centimeter, D the degree of ionization, n_e the electron number density in electrons per cubic centimeter, and T the temperature in electron volts. Since the maximum temperature computed in the Eulerian program was approximately 2 eV (and further, because the program used the Saha equation for singly ionized species in the derivation of the electron number density), the degree of ionization was taken to be one. Next, the radiation from the LSD wave was assumed to be isotropic, emanating from a homogeneously radiating spherical source. The center of this source was taken to be the centroid of the radiating LSD wave located at a distance $Z(t)$ above the surface given by

$$Z(t) = \underset{\substack{\text{vol}\\ \text{of LSD}}}{\oint} z(t)\dot{f}\,dV \Big/ \underset{\substack{\text{vol}\\ \text{of LSD}}}{\oint} \dot{f}\,dV \tag{13}$$

Finally, the radiative energy flux $\dot{Q}_R(r,t)$, where r is the radial distance on the target from the center of the beam, was computed by

$$\dot{Q}_R(r,t) = \left(\underset{\substack{\text{vol}\\ \text{of LSD}}}{\oint} \dot{f}\,dV\right)(\cos\phi/4\pi R^2) \tag{14}$$

where $R^2 = Z^2 + r^2$ and $\cos\phi = Z/R$.

The second estimate was made by assuming that the plasma was pseudo-optically thick, i.e., the energy flux per unit area of the plasma was assumed to be some fraction of a 23,000 K blackbody radiator, consistent with that observed in Ref. 4. Thus,

$$\dot{Q}_s = w\sigma T^4 \tag{15}$$

where $\dot{Q}_s$ is the radiative flux per unit area of the plasma surface, w the fractional multiplier to bring the flux in line with Ref. 4, and σ the Stefan-Boltzmann constant. In order to compute the energy to the target as a function of time and radial location on the target, the flux given by Eq. (15) was multiplied by the area of the plasma disk A_p, assumed to be the cross-sectional area of the laser beam, and the view factor from the plasma to the annular area corresponding to the radius of interest. Thus, the flux to the target as a function of time and radial location $\dot{Q}_R$ is given by

$$\dot{Q}_R(t,r) = (A_p/A_r)F_{p-t}\dot{Q}_s \tag{16}$$

where A_r is the annular target area and F_{p-t} the view factor.

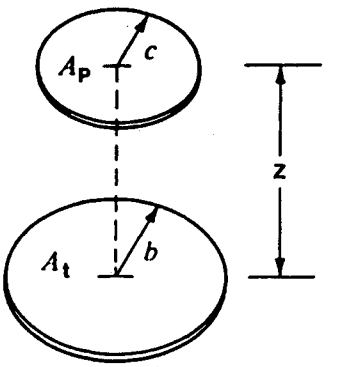

Fig. 6 Nomenclature for Eqs. (17) and (18).

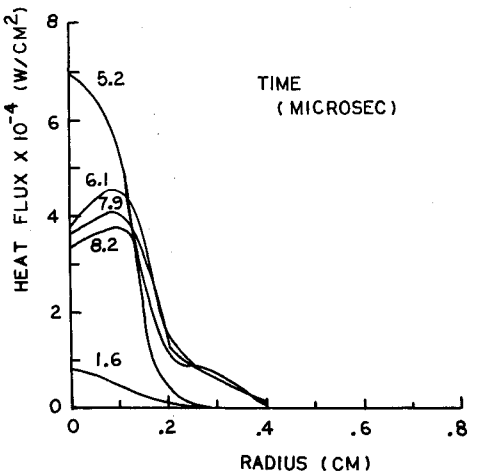

Fig. 7 Computed time evolution of the radial distribution of energy flux to the target due to convective heat transfer.

The view factor to a particular annular ring on the target was obtained by computing the view factor from the plasma to the area of the target from the center of the beam to the outside diameter of the annular ring and subtracting the view factor from the plasma to the target from the center of the beam to the inside diameter of the annular ring. The view factor from the plasma to a circular target area of radius b (see Fig. 6) is given by[20]

$$F_{p-A} = (A_t/A_p)[(1/2B^2)(X - \sqrt{X^2 - 4B^2C^2})] \tag{17}$$

where A_t is the area of the target from the center of the beam to radius of interest and B, C, and X are given by

$$B = b/Z,\ C = c/Z$$

$$X = 1 + B^2 + C^2 \tag{18}$$

where b, c, and Z are pertinent dimensions as illustrated in Fig. 6.

V. Results

Convective Heat Transfer

Figure 7 gives the time evolution and radial distribution of the convective heat transfer. It is clear that the convective heat transfer is confined to a fairly small radial region on the target compared to that of the Maher and Hall experiment (Fig. 1) and declines rapidly after approximately 5 μs.

Radiative Heat Transfer

The radiative contribution to the enhanced coupling computed assuming optically thin plasma [i.e., Eqs. (12-14)] yielded a negligible amount of heat transferred to the target (less than 1% of the beam energy), in agreement with previous studies.[5,17] The results of the pseudo-optically thick assump-

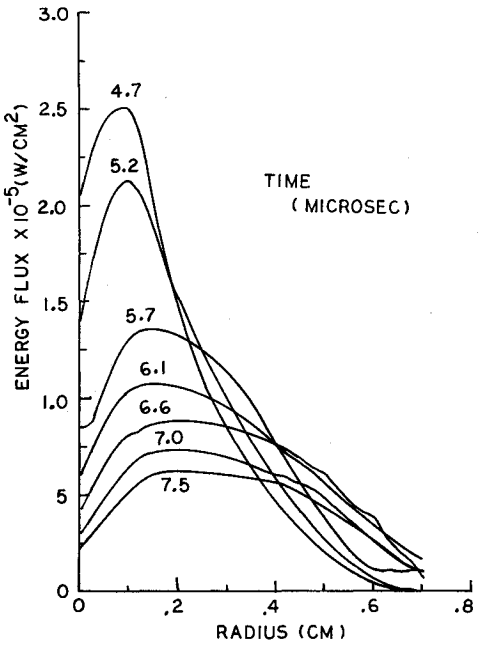

Fig. 8 Computed time evolution of the radial distribution of energy flux to the target due to vapor condensation.

tion [i.e., Eqs. (15–18)] also yield negligible contributions to the thermal coupling; however, because the reported findings of Ref. 4 have been cited as experimental evidence in conflict with this statement, we shall address the Ref. 4 findings further.

With regard to the Ref. 4 experiments, it should be recognized that the time of a typical experiment was reported to be 3.46 μs. The average energy density (pulse fluence) of the laser pulse was reported to be approximately 17 J/cm^2 and the estimated plasma-radiated energy transported to the target was reported to be approximately 0.98 J/cm^2. Two things should be noted: 1) Ref. 4 was dealing with a laser-supported combustion wave rather than an LSD wave (this is consistent with the reported laser flux, because the average flux would be only 5×10^6 W/cm^2, which is below the threshold of ignition for an LSD wave on aluminum targets of $\approx 10^7$ W/cm^2, see, e.g., Ref. 3) and 2) because of the large beam radius used in Ref. 4 and the short time of the experiments (3.46 μs as opposed to the 20+ μs in the Maher and Hall experiment), the view factor need not be considered because it was ≈ 1.0. With these facts in mind, it is possible to estimate that the radiative emission from the plasma of Ref. 4 is approximately 18% of that for a 23,000 K blackbody emitter. This estimate is also in agreement with the published emission curves in Ref. 4.

Using an 18% blackbody radiation factor, assuming the lowest flux that can support an LSD wave (i.e., 10^7 W/cm^2), and assuming no influence due to considerations of the view factor, the maximum irradiation of the target due to radiative emissions from the plasma of a 23,000 K blackbody emitter is only $\approx 2.9\%$ of the laser flux (i.e., a 23,000 K blackbody emitter radiates at 16% of the 10^7 W/cm^2 that would be in the incoming beam; 18% of this 16% yields the 2.9%). Because an LSD wave is essentially 100% shielding to the laser flux, laser fluxes greater than 10^7 W/cm^2, as in the Maher and Hall experiment,[1] yield an even lower percent coupling; thus, 2.9% represents a maximum coupling to the target due to plasma reradiation in the cases where LSD waves are ignited. Futher, this maximum coupling assumes that the reradiated emission is not attenuated by the intervening gas and that it is absorbed by the target at 100%. If view factor considerations are taken into account, the maximum coupling coefficient due to radiation for a 10^7 W/cm^2 beam drops to 2.3% for the size target used in the Maher and Hall experiment, even without taking into account absorption by the intervening gas. In fact, such absorption must be considered because, for the Maher and Hall experiment, the plasma is several target diameters from the target after 20 μs. Thus, even the pseudo-optically thick method of approximating the radiation contribution to the thermal coupling for the Maher and Hall experiment yields a coupling of less than 1%.

Vapor Condensation

Computations of the predicted energy transfer back to the target by vapor condensation were made according to Eqs. (10) and (11), assuming an absorptivity of 100% for the purpose of vapor evolution (cf Sec. VI). The results in a form similar to those for convective heat transfer are shown in Fig. 8. A comparison with Fig. 7 demonstrates two points: 1) the potential for transferring energy to the target is considerably greater than that for convective heat transfer and 2) the radial distribution of that energy is more in line with the Maher and Hall experiment. Further, for the reasons discussed earlier, the results for condensation are considered to underestimate what actually occurs. It should be kept in mind that these results assume that sufficient vapor was evolved from the target in the early phases of the pulse (≈ 4 μs) to account for the vapor being available for recondensation. (It should be noted that the Maher-Hall pulse shape, cf Fig. 1, does not demonstrate a large gain-switch spike that might be anticipated by the reader.) In this regard and as noted above, the calculations were made assuming that the absorptivity (or apparent absorptivity) of the target builds rapidly to nearly 100% in the very early times of the pulse. Support for this contention will be discussed in Sec. VI.

Under the assumption of near 100% absorptivity while the beam is not shielded by the LSD wave, Fig. 9 shows the evolution and transport of the target vapor as a function of time as computed using the Eulerian program. Also shown are the pressure contours for the same selected times. It can be seen that the vapor evolves, is transported away from the target, and then forced back down onto the target by the overpressures produced by the LSD wave; this is the exact requirement to make the mechanism viable.

It is also possible to determine the depth of the hole produced by the evolving vapor, as well as the hole/mound after the vapor has recondensed onto the target out to 10 μs; these are shown in Fig. 10. It should be noted that the amounts of condensed vapor that would be noticeable outside the beam radius is very slight, less than 1 μm in thickness at the maximum height.

Summary of Results

Because of grid size limitations, the computations performed for this study were only taken out to 10 μs; however, the trends are evident. Figure 11 shows the results of accumulated energy density (i.e., J/cm^2) out to 10 μs for convective heat transfer, vapor condensation, and the sum of convection and condensation, along with the Maher and Hall data. It should be noted that, although the curve is less than that of the Maher and Hall data, the experimental curve represents that for the entire experiment and the computed curve begins to approach that of the experiment. In fact, at the 10 μs point, the beam energy was accumulated to approximately 5 J, while the area under the combined convection-condensation curve represents 0.715 J. Thus, at the 10 μs point, the coupling coefficient is approximately 14.3%, compared to 17.5% for the experiment. A more important comparison is that the computed radial distribution of the energy is in very good agreement with experiment, an agreement that cannot be reproduced by either convective or radiative heat-transfer calculations even if the magnitudes of such calculations are assumed to be way off on the low side.

VI. Discussion of Near 100% Absorptivity

The calculations for enhanced coupling due to vapor condensation assumed that 100% of the laser energy getting to the target (i.e., not shielded by the LSD/air-breakdown plasma) went into evolving target vapor (cf above). This means that

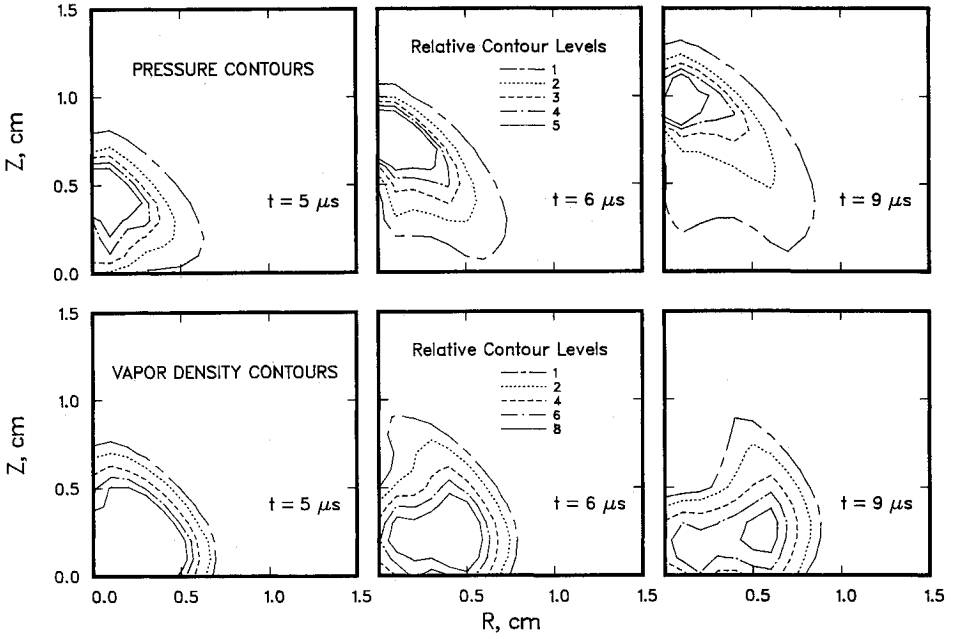

Fig. 9 Computed pressure and vapor-density contours for the Maher and Hall experiment. Calculation assumes a high absorptivity in the early times of the pulse for the purpose of vapor evolution. (Numbers associated with contours indicate multiples of 2 atm and 4×10^{-5} g/cm^3 for the pressure and vapor-density contours, respectively.)

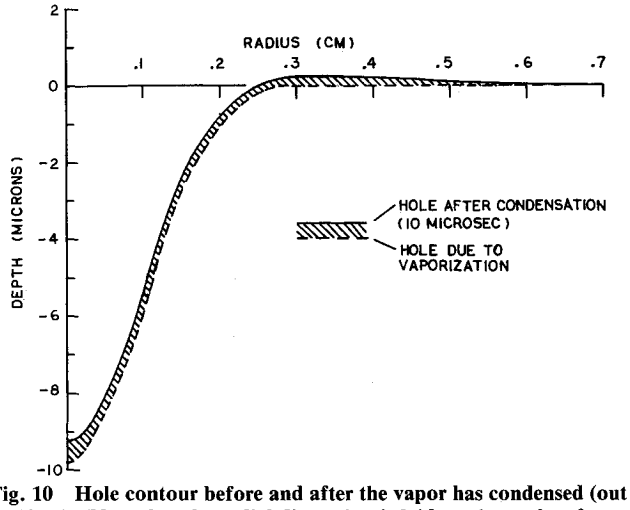

Fig. 10 Hole contour before and after the vapor has condensed (out to 10 μs). (Note that the radial dimension is laid out in tenths of centimeters, while the hole depth is in micrometers; thus, the hole depth is exaggerated by three orders of magnitude.)

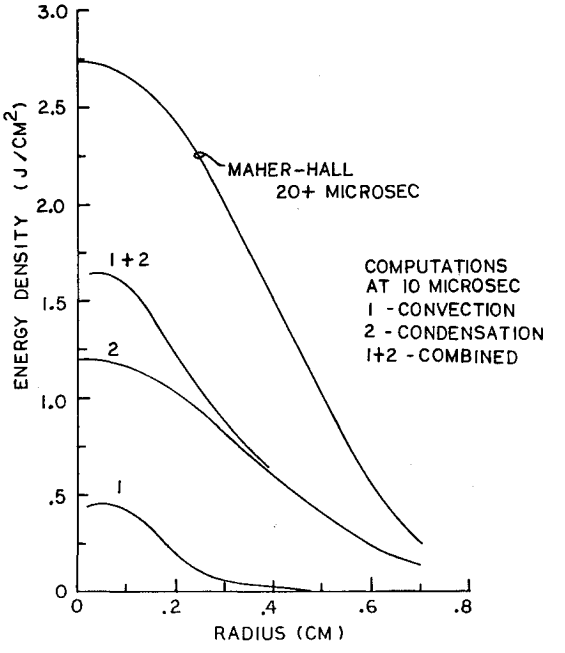

Fig. 11 Summary of energy density vs radial position results from computations after 10 μs for convection, condensation, and combined convection and condensation. Also shown is the Maher and Hall experimental result.

essentially the entire energy of the beam in the first 4–5 μs was captured by the vapor. This energy represents 39–43% of the energy in the pulse (cf Fig. 1). Our calculations indicate that less than 20% of this vapor has recondensed onto the target by 10 μs. Thus, we may conclude that, if we assume 100% of the unshielded beam goes into evolving vapor, sufficient energy is captured by the vapor and redeposited onto the target in the proper radial distribution, via condensation, to explain most of the enhanced thermal coupling demonstrated experimentally. On the other hand, this cannot be said about the mechanisms of convective and radiative heat transfer. So in this sense, the notion of a high apparent absorptivity for the purpose of vapor evolution appears to be compatible with the observed enhanced coupling. It should be noted that we have intentionally been conservative in our calculations of both the rate of impingement and the energy flux into the target given in Eq. (11); accordingly, the more mass/energy per mass deposited in the target, the less evolved vapor is needed. Thus, while the computation requires a large absorptivity, it need not be as high as we have used.

With this caveat in mind, let us discuss the question, "Is there any other evidence that aluminum surfaces suddenly reach a threshold above which the apparent absorptivity becomes large?" By apparent absorptivity, we mean the ability of the laser beam to evolve vapor. We think that such evidence does exist, though normally associated with vacuum experiments. For example, Ready[21] (especially pp. 109–116) discusses the reduction of reflectivity when laser irradiance reaches a material/laser-wavelength-dependent critical threshold flux. Above such thresholds, the target materials exhibit apparent absorptivities of nearly 1.0. Ready[21] associates this increase in apparent absorptivity to target vapor formation and absorption of the incident radiation by the ionized vapor. Discussions of apparent absorptivities of near 1.0 are also noted by DeMichelis,[22] again attributed to the presence of target vapor.

That this absorptivity by the vapor is directly coupled into the target and goes into the evolution of more vapor has also been proposed in the literature. Ready[21] suggests that such is the case, but does not provide an explanation for the mechanism. Schwirzke,[23] on the other hand, not only suggests that the vapor is responsible for the experimentally observed increase in apparent absorptivity, but also suggests a mechanism for efficiently coupling the vapor-absorbed energy directly into the target. In turn, such coupling evolves additional vapor, thereby sustaining the process. The absorption process is that discussed by Dawson[19] and requires a critical vapor number density. For 10.6 μm radiation, this critical number density is approximately 10^{19} vapor atoms per cubic centimeter, assuming single ionization. In a separate reference Schwirzke,[24] suggests the same process is valid in the presence of atmospheric pressure.

In fact, if the laser flux is sufficiently high to produce vapor at a rate larger than the diffusional processes can move it away from the surface, then the vapor density will be that consistent with the vapor partial pressure being equal to that of the surrounding atmosphere. Thus, above some flux (but less than that required to ignite an LSD wave), the atmospheric pressure provides a lower bound on the number density of the vapor; at 1 atm and at the vaporization temperature of aluminum, the vapor number density will be approximately one-third of the critical number density required by the Dawson/Schwirzke mechanism. Thus, the threshold flux need be only that sufficient to provide the additional vapor density required to reach the critical density. This would suggest that the critical flux should be pressure dependent, increasing with decreasing pressure. If we can make the connection of this "critical breakdown" and subsequent catastrophic apparent absorptivity increase to the threshold for ignition of an LSD, then the Hall et al.[25] work can be interpreted as evidence in favor of this mechanism. It is interesting to note that Root[3] seems to hint at this same increase in apparent absorptivity for 3.8 μm laser experiments, although he carefully disconnects this from the 10.6 μm experiments.

VII. Conclusions

In this paper, we have presented the results of computations for convective and radiative heat transfer to an aluminum target for the case where a laser-supported detonation (LSD) wave is ignited by 10.6 μm laser radiation. The Maher and Hall[1] 9.3 J experiment was used for comparison. These results indicate that combined convection and plasma reradiation do not appear to provide sufficient energy coupling to the target to explain the 17.5% thermal coupling observed in the experiment. Not only does the amount of energy fall far short of that required to explain the observed coupling, but the radial distribution of the convection/radiation-coupled energy does not match that observed. One must conclude that some other mechanism(s) is responsible for the observed coupling.

Vapor recondensation was also explored as a possible mechanism for explaining the observed coupling. The results of computations modeling condensation appear to be in close agreement with both the observed coupling coefficient and radial distribution of target-deposited energy. A prerequisite for viability of such a mechanism, however, is that the laser couples to the target with a large apparent absorptivity for the purpose of vapor evolution in the early times of the pulse. Corroborating evidence that this might be the case was also presented.

This paper has not attempted to "prove" that vapor condensation is responsible for the observed thermal coupling of the Maher and Hall experiment, but rather to suggest that such a notion has a rational basis. We believe the ramifications (of the possibility that the condensation mechanism contributes to the observed coupling) are sufficiently great that it should be given further attention. Some of the ramifications are obvious; for example, it may provide the key to understanding the link between short- and long-wavelength experiments. Further, it may also provide the connection between vacuum and atmosphere experiments. And finally, if correct, it would tend to suggest that the important physics to be concentrated on is not the gasdynamics of the flow/plasma for the LSD, but rather the mechanisms at work in the very early times of the pulse.

Acknowledgment

The authors gratefully acknowledge the assistance and contributions of Dr. J. E. Hitchcock, Department of Aeronautics and Astronautics, Air Force Institute of Technology.

References

[1]Maher, W. E. and Hall, R. B., "Experimental Thermal Coupling of Laser Beams," *Journal of Applied Physics*, Vol. 49, April 1978, pp. 2254–2261.

[2]McKay, J. A. et al., "Pulsed-CO_2-Laser Interaction with Aluminum in Air: Thermal Response and Plasma Characteristics," *Journal of Applied Physics*, Vol. 50, May 1979, pp. 3231–3240.

[3]Root, R. G., "Laser Interaction: Thermal and Mechanical Coupling to Targets," *Journal de Physique (Paris) Colloque C9,* Vol. 41, Nov. 1980, pp. C9-59—C9-73.

[4]Mitchell, R. W., Conrad, R. W., Roy, E. L., Keefer, D. and Mathews, W., "Role of Radiative Transfer in Pulsed-Laser-Plasma-Target Interactions," AIAA Paper 78-139, Jan. 1978.

[5]Jackson, J. P. and Jumper, E. J., "Mechanisms of Enhanced Coupling by a Pulsed Laser," *Laser Digest*, AFWL-TR-75-229, 1975, pp. 172–184.

[6]Jumper, E. J., "Enhanced Thermal Coupling by Repetitively-Pulsed Lasers," *Laser Digest*, AFWL-TR-76-229, 1976, pp. 161–174.

[7]Nielsen, P. E., "Hydrodynamic Calculations of Surface Response in the Presence of Laser-Supported Detonation Waves," *Journal of Applied Physics*, Vol. 46, Oct 1975, pp. 4501–4505.

[8]Couick, J. R., "Enhanced Thermal Coupling by a Repetitively Pulsed Laser," Thesis, Air Force Institute of Technology, Wright-Patterson AFB, OH, Rept. AFIT/GAE/AA/85M-3, March 1985.

[9]Nielsen, P. E. and Jackson, J. P., "Intense Laser-Solid Interactions," *Aeronautics Digest*, Rept. USAFA-TR-80-7, April 1980, pp. 47–64.

[10]Eckert, E.R.G., "Survey of Boundary Layer Heat Transfer at High Velocities and High Temperature," WADC Tech. Rept. 59–624, April, 1960.

[11]Eckert, E.R.G. and Drake, R. M. Jr., *Analysis of Heat Transfer*, McGraw-Hill, New York, 1972.

[12]Eckert, E.R.G., "Engineering Relations for Heat Transfer and Friction in High Velocity Laminar and Turbulent Boundary-Layer Flow over Surfaces with Constant Pressure and Temperature," *Transactions of ASME*, Vol. 78, Aug. 1956, pp. 1273–1283.

[13]Schlichting, H., *Boundary-Layer Theory*, 6th ed., McGraw-Hill, New York, 1968.

[14]Walters, C. T., Barnes, R. H., and Beverly, R. E., III, "Initiation of Laser-Supported-Detonation (LSD) Waves," *Journal of Applied Physics*, Vol. 49, May 1978, pp. 2937–2949.

[15]Levine, J. D. and Gyftopoulos, E. P., "Adsorption Physics of Metals Partially Covered by Metallic Particles. II Desorption Rates of Atoms and Ions," *Surface Science*, Vol. 1, 1964, pp. 225–241.

[16]Vincenti, W. G. and Kruger, C. H. Jr., *Introduction to Physical Gas Dynamics*, Robert E. Krieger Publishing Co., 1977.

[17]Stamm, M. R., Nielson, P. E. and Jackson, J. P., "Radiative Coupling in Laser-Target Interactions," *Laser Digest*, AFWL-TR-74-241, 1974, pp. 163–169.

[18]Jackson, J. P. and Nielsen, P. E., "Role of Radiative Transport on the Propagation of Laser Supported Combustion Waves," *AIAA Journal*, Vol. 12, Nov. 1974, pp. 1498–1501.

[19]Dawson, J. M., "On the Production of Plasma by Giant Pulse Lasers," *The Physics of Fluids*, Vol. 7, July 1964, pp. 981–987.

[20]Wong, H. Y., *Handbook of Essential Formulae and Data on Heat Transfer for Engineers*, Longman, London, 1977.

[21]Ready, J. F., *Effects of High-Power Laser Radiation*, Academic Press, New York, 1971.

[22]DeMichelis, C., "Laser Interaction with Solids—A Bibliographical Review," *IEEE Journal of Quantum Electronics*, Vol. QE-6, Oct. 1970, pp. 630–641.

[23]Schwirzke, F., "Unipolar Arc Model," *Journal of Nuclear Materials*, Vols. 128 & 129, 1984, pp. 609–612.

[24]Schwirzke, F., "Unipolar Arching, a Basic Laser Damage Mechanism," Naval Postgraduate School, Monterey, CA, Rept. NPS-61-83-008, May 1983.

[25]Hall, R. B., Maher, W. E., and Wei, P.S.P., "Laser Effects at 10.6 Microns," *Laser Beam Target Interaction*, Vol. II, U.S. Air Force Weapons Laboratory, NM, Rept. AFWL-TR-75-342, July 1976.